Broad-Band Wavelength Conversion Based on Cross-Gain Modulation and Four-Wave Mixing in InAs–InP Quantum-Dash Semiconductor Optical Amplifiers Operating at 1550 nm

A. Bilenca, *Student Member, IEEE*, R. Alizon, *Student Member, IEEE*, V. Mikhelashhvili, D. Dahan, *Student Member, IEEE*, G. Eisenstein, *Fellow, IEEE*, R. Schwertberger, D. Gold, J. P. Reithmaier, *Member, IEEE*, and A. Forchel, *Associate Member, IEEE*

***Abstract*—Wavelength conversion based on four-wave mixing (FWM) and cross-gain modulation (XGM) is experimentally demonstrated for the first time in a 1550-nm InAs–InP quantum-dash semiconductor optical amplifier. Continuous-wave FWM with a symmetric conversion efficiency dependence on detuning direction and FWM mediated short-pulse wavelength conversion are demonstrated. Using XGM, we have successfully implemented short-pulse wavelength conversion over 10 THz and error-free data conversion of a 2.5-Gb/s data sequence over 7.5 THz. The pulsed XGM experiments suggest that adjacent regions within an inhomogeneously broadened gain spectrum are partially coupled which increases the operational bandwidth, but at the expense of speed.**

***Index Terms*—Nonlinear optics, optical amplifiers, optical communication, quantum dots, semiconductor lasers.**

I. Introduction

SEMICONDUCTOR optical amplifiers (SOAs) have become the nonlinear media of choice for most signal processing devices [1] needed in future broad-band all-optical networks. Quantum-well (QW) and bulk SOAs, in which the processes of cross-gain modulation (XGM), cross-phase modulation (XPM), and four-wave mixing (FWM) are employed, have been demonstrated in numerous experimental applications [1], [2]. The modest optical bandwidth of QW and bulk SOAs limits the spectral region over which XGM and XPM can be used while the gain dynamics determines the maximum data and switching rates [1]. The process of FWM offers the advantage of data format independence and flexible conversion schemes, but in QW and bulk SOAs there exists an inherent asymmetry in conversion efficiencies between shorter and longer wavelengths. The asymmetry stems from interference among the various nonlinear mechanisms which mediate the FWM process [3] and is directly related to the linewidth enhancement factor (α-parameter).

Manuscript received October 21, 2002; revised December 19, 2002. This work was supported by the European Community under Project BigBand of the IST. The work of A. Bilenca and D. Dahan was supported by the Israeli Ministry of Science.

A. Bilenca, R. Alizon, V. Mikhelashhvili, D. Dahan, and G. Eisenstein are with the Electrical Engineering Department, Technion, Haifa 32000, Israel (e-mail: gad@ee.technion.ac.il).

R. Schwertberger, D. Gold, J. P. Reithmaier, and A. Forchel are with the Technische Physik, Universitat Wurzburg, Wurzburg 97074, Germany.

Digital Object Identifier 10.1109/LPT.2003.809281

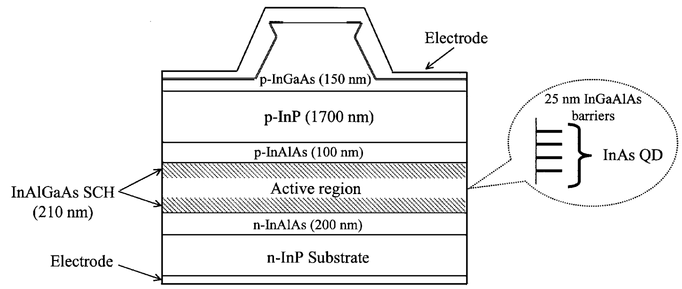

Fig. 1. Structure of the 1550-nm InAs–InP QD SOA.

Many limitations of QW and bulk SOAs can be overcome by application of quantum-dot and quantum-dash (QD) SOAs. QD SOAs with large bandwidths have been demonstrated in both InAs–GaAs [4], [5] and InAs–InP SOAs [6]. Ultrafast gain dynamics have been seen in pump probe examinations [7], [8] and XGM with 10 Gb/s has been demonstrated proving the potential of QD SOAs for high-speed XGM-based converters [9]. Furthermore, symmetric, i.e., detuning direction-independent, FWM conversion efficiencies were reported in QD SOAs [5], [6], [10] indicating a low α-parameter and suggesting superior wavelength conversion capabilities.

The results obtained using InAs–GaAs QD SOAs operating at 950–1300 nm shed significant light on the physical properties of QD gain media [5] but it is obvious that in order to have a major impact on fiber-optics communication, QD SOAs operating at 1550 nm must be implemented. We have recently reported linear and nonlinear characteristics of the first InAs–InP 1550-nm QD SOA [6] and in this letter, we present dynamical investigations aimed at exploiting the broad-band gain spectrum and fast gain dynamics of those 1550-nm QD SOAs using both FWM and XGM.

II. Experimental Results and Discussion

The QD SOA used in the experiments is similar to the one described in [6] and is shown schematically in Fig. 1. It is based on a standard separate confinement heterostructure with an active region comprising four quantum-dash layers of five mono-

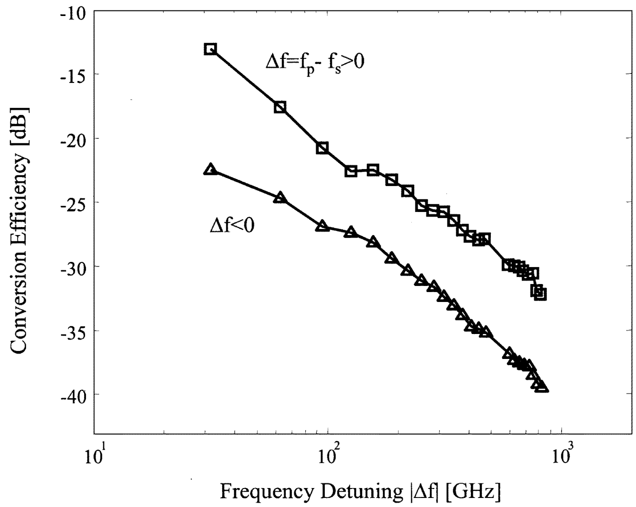

(a)

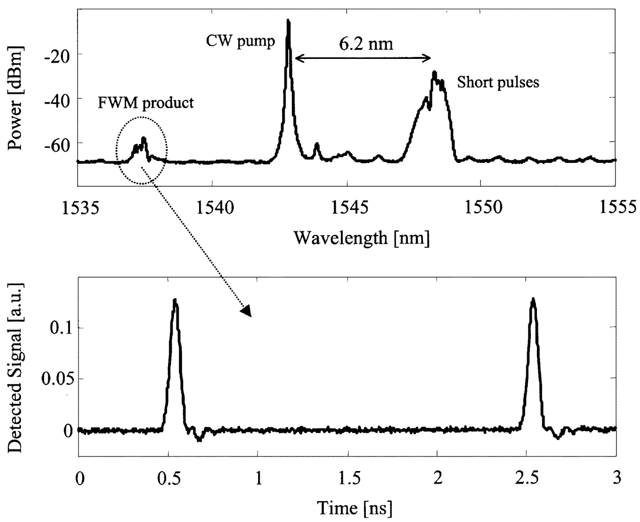

(b)

Fig. 2. FWM experiments. (a) CW FWM conversion efficiency dependence on detuning frequency. (b) Wavelength conversion of 40-ps pulses at a 6.2-nm detuning optical spectrum and time-domain description.

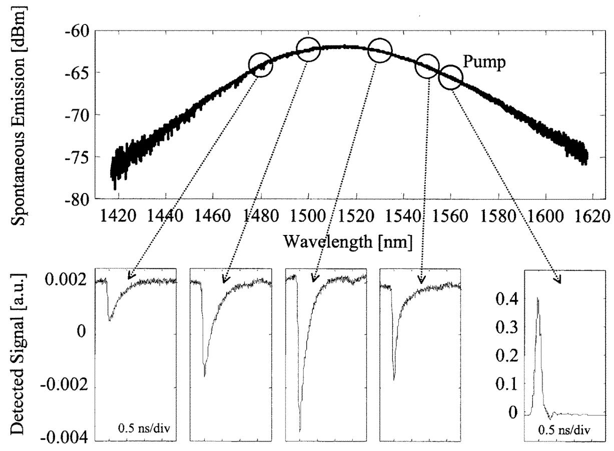

(a)

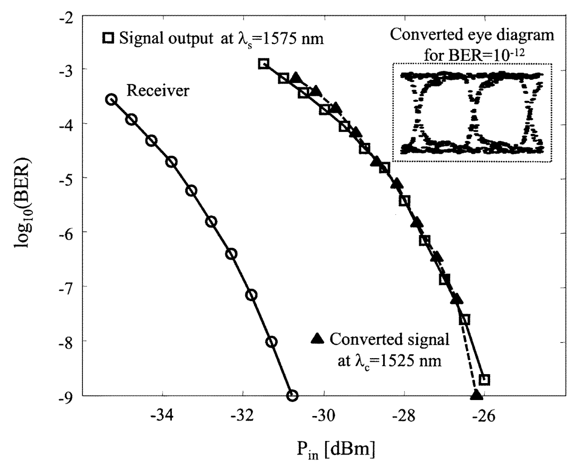

(b)

Fig. 3. XGM experiments. (a) Wavelength conversion of 40-ps pulses at 1560 nm with conversion detunings of up to 80 nm. Spontaneous emission spectrum and time-domain description are shown. (b) BER measurements of 2.5-Gb/s pseudorandom data at a 50-nm detuning.

layers thickness each separated by 25-nm-wide InAlGaAs barriers [11]. The SOA has a ridge waveguide structure that is 2.5 μm wide and 2.1 mm long and a residual facet reflectivity of 0.01%. The gain bandwidth measured at 10 dB below the peak was approximately 180 nm and the unsaturated gain was 12 dB at a current bias of 160 mA.

A. Nondegenerate FWM Experiments

Continuous-wave (CW) nondegenerate FWM measurements were performed with a pump signal fixed at 1542 nm and a tunable probe whose frequency was scanned by more than $\pm$1000 GHz. The pump and probe input power levels were, respectively, 0 and -11 dBm. Fig. 2(a) shows the FWM conversion efficiency of the conjugate FWM product for both conversion directions, i.e., positive and negative detunings. The two efficiency curves have the same shape, namely, the asymmetry between conversion directions common in QW and bulk SOAs is not observable. This is attributed to the reduction in the α parameter, consistent with [6], [10]. Additional experiments we performed on quantum-dash lasers having identical structures yield wavelength dependent α-parameters of 2–3.5 and similar values were reported in [12]. The difference in absolute efficiencies is most likely due to the slope of the gain spectrum at the relevant wavelength range.

FWM-mediated wavelength conversion of short pulses is described in Fig. 2(b). In this case, the probe signal was a train of 40-ps-wide pulses at a repetition rate of 500 MHz and an average input power of -7 dBm. The wavelength of the pulses was detuned from the CW pump by 6.2 nm. The converted product was filtered, detected and displayed by a fast oscilloscope. We note the very fast transitions of the converted pulse and its large signal-to-noise ratio.

B. XGM Experiments

Several XGM experiments using short pulses as well as nonreturn–to-zero (NRZ) data streams were also performed. Wavelength conversion of short pulses was used to estimate the possible wavelength span over which conversion is possible. Pulses of 40-ps duration at 1560 nm with a peak power of $+12$ dBm were used for the pump while a tunable probe scanned the gain spectrum in 10-nm steps. Fig. 3(a) shows four converted pulses at detunings of $\Delta\lambda = 10$, 30, 60, and 80 nm. Reasonably large efficiencies yielding converted pulses with a high signal-to-noise ratio are observed at detunings of up to 80 nm (10 THz). For a larger detuning, $\Delta\lambda \sim 100$ nm, the conversion efficiency reduced dramatically and the detected pulses all but diminished.

The magnitude and temporal shape of each pulse depends on the respective conversion efficiency and gain dynamics at the converted wavelengths. The temporal response of all pulses has a general form that shows fast gain saturation followed by two gain recovery mechanisms, one fast and the other slow. The response can be fitted to a simple sum of two exponents, i.e., $-C_{\rm fast}e^{-t/\tau_{\rm fast}} - C_{\rm slow}e^{-t/\tau_{\rm slow}}$. The observed initial time constant $\tau_{\rm fast}$ is of the order of 20 ps for all pulses. This is an artificial observation since it is limited by the detection bandwidth. The second time constant $\tau_{\rm slow}$ is approximately 300 ps in all cases. The constants $C_{\rm slow}$ and $C_{\rm fast}$ represent the relative significance of the two recovery processes. For $\Delta\lambda$ of 10 and 20 nm [not shown in Fig. 3(a)], $C_{\rm fast} \approx 0.002$ and $C_{\rm slow} \approx 0.002 - 0.003$. For $\Delta\lambda = 30$ nm, $C_{\rm fast} \approx 0.0005$, and $C_{\rm slow} \approx 0.0056$. For large detunings, $C_{\rm fast}$ is smaller than 0.0003 and $C_{\rm slow}$ varies from 0.003 to 0.006. The data in Fig. 3(a), together with the result of the parameter fit, clearly differentiate between small and large detunings. For $\Delta\lambda =$10 and 20 nm, $C_{\rm fast}$ is large and the recovery is dominated by $\tau_{\rm fast}$. These two cases represent XGM within the estimated homogeneously broadened gain region. For large detunings, $C_{\rm fast}$ is vastly reduced and the observed response is dominated by $\tau_{\rm slow}$.

The carrier and gain dynamics governing the response of quantum-dash structures are not known in detail. While quantum dashes are predicted to be similar to the more developed quantum dots, their elongated structures [11] are likely to result in some differences. These have not been studied in detail, neither theoretically nor in experiments. However, published data on quantum-dash lasers and amplifiers [6], [12] suggest that their optoelectronic characteristics do not differ much from those of quantum dots. In the present experiments, we examined eight converted pulses at successively increasing $\Delta\lambda$ which enables us to qualitatively explain the main features of the gain dynamics. Within the homogeneously broadened gain spectrum, the gain dynamics are very fast. The observed time constant $\tau_{\rm fast}$ is unresolved here, but its real value can be estimated from published pump-probe data in GaAs quantum-dot SOAs [7]–[9] to be a few picoseconds. The pulsed FWM response, Fig. 2(a), where $\Delta\lambda = 6.2$ nm is also consistent with fast dynamics as is XGM of 10-Gb/s data converted over $\Delta\lambda$ smaller than 15 nm reported in [9].

For large detunings, $C_{\rm fast}$ is vastly reduced and the observed response is dominated by $\tau_{\rm slow}$. The XGM response involves, in this case, coupling between tails of adjacent spectral regions within an inhomogeneously broadened gain spectrum. This coupling stems from complex carrier injection mechanism involving the wetting and barrier layers through which the different dash populations are fed [13], [14]. Carrier emission rates to the pseudocontinuous wetting or barrier levels increase with energy [13], thereby slowing the gain recovery time at large detunings on the short wavelength side. Intradot coupling, a process whose dynamics also slow with the detuning [5], is an additional possible mechanism allowing for XGM over large wavelength spans. A widened XGM operational bandwidth comes, therefore, at the expense of speed and hence large detuning and data rate have to be traded off against each other.

XGM was demonstrated with 2.5-Gb/s NRZ data and a very large detuning of 50 nm (7.5 THz). The average power coupled into the SOA was in this case 4 and -10 dBm for the signal $(\lambda_s = 1575~\text{nm})$ and CW probe $(\lambda_c = 1525~\text{nm})$, respectively. Fig. 3(b) shows the bit-error-rate (BER) curves measured at the SOA output of the signals at the original and converted wavelengths. The two curves are identical indicating that the conversion process did not deteriorate the data. The $\sim$5-dB penalty relative to the receiver BER curve is due to added noise. The inset shows a clear and open eye diagram of the converted signal. The relatively moderate bit rate of 2.5 Gb/s was easily converted at the large detuning of 50 nm. At 10 Gb/s and for the same $\Delta\lambda = 50$ nm, the amplifier proved to be too slow.

REFERENCES

[1] T. Durhuus, B. Mikkelsen, C. Joergensen, S. Lykke Danielsen, and K. E. Stubkjaer, "All-optical wavelength conversion by semiconductor optical amplifiers," *J. Lightwave Technol.*, vol. 14, pp. 942–954, June 1996.

[2] R. Ludwig and G. Raybon, "BER measurements of frequency converted signals using four wave mixing in semiconductor optical amplifier at 1, 2.5, 5 and 10 Gbit/s," *Electron. Lett.*, vol. 30, pp. 338–339, 1994.

[3] K. Kikuchi, M. Kakui, C.-E. Zah, and T.-P. Lee, "Observation of highly nondegenerate FWM in 1.5 mm traveling-wave semiconductor optical amplifiers and estimation of nonlinear gain coefficient," *IEEE J. Quantum Electron.*, vol. 28, pp. 151–156, Jan. 1992.

[4] T. Akiyama, H. Kuwatsuka, T. Simoyama, Y. Nakata, K. Mukai, M. Sugawara, O. Wada, and H. Ishikawa, "Nonlinear gain dynamics in quantum-dot optical amplifiers and its application to optical communication devices," *IEEE J. Quantum Electron.*, vol. 37, pp. 1059–1065, Aug. 2001.

[5] Y. Nambu, A. Tomita, H. Saito, and K. Nishi, "Effects of spectral broadening and cross relaxation on the gain saturation characteristics of quantum dot laser amplifiers," *Jpn. J. Appl. Phys.*, vol. 38, pp. 5087–5095, 1999.

[6] A. Bilenca, R. Alizon, V. Mikhelashvili, G. Eisenstein, R. Schwertberger, D. Gold, J. P. Reithmaier, and A. Forchel, "InAs/InP 1550-nm quantum-dash semiconductor optical amplifiers," *Electron. Lett.*, vol. 38, pp. 1350–135, 2002.

[7] J. Feldmann, S. T. Cundiff, M. Arzberger, G. Böhm, and G. Abstreiter, "Carrier capture into InAs/GaAs quantum dots via multiple optical phonon emission," *J. Appl. Phys.*, vol. 89, pp. 1180–1183, 2001.

[8] T. Akiyama, T. Shimoyama, H. Kuwatsuka, Y. Nakata, K. Mukai, M. Sugawara, O. Wada, and H. Ishikawa, "Gain nonlinarity and ultrafast carrier dynamics in quantum dot optical amplifiers," in *ECOC 1999*, vol. II, pp. 76–77.

[9] T. Akiyama, N. Hatori, Y. Nakata, H. Ebe, and M. Sugawara, "Wavelength conversion based on ultrafast $(<3~\text{ps})$ cross gain modulation in quantum-dot optical amplifiers," presented at the ECOC 2002, Copenhagen, Denmark, Paper 4.3.7.

[10] T. Akiyama, H. Kuwatsuka, N. Hatori, Y. Nakata, H. Ebe, and M. Sugawara, "Symmetric highly efficient $(\sim 0~\text{dB})$ wavelength conversion based on four wave mixing in quantum dot optical amplifiers," *IEEE Photon. Technol. Lett.*, vol. 14, pp. 1139–1141, Aug. 2002.

[11] R. Schwertberger, D. Gold, J. P. Reithmaier, and A. Forchel, "Long-wavelength InP-based quantum-dash lasers," *IEEE Photon. Technol. Lett.*, vol. 14, pp. 735–738, June 2002.

[12] A. A. Ukhanov, R. H. Wang, T. J. Rotter, A. Stintz, L. F. Lester, P. G. Eliseev, and K. J. Malloy, "Orientation dependence of the optical properties in InAs quantum-dash lasers on InP," *Appl. Phys. Lett.*, vol. 81, pp. 981–983, 2002.

[13] D. G. Deppe and D. L. Huffaker, "Quantum dimensionality, entropy and the modulation response of quantum dot lasers," *Appl. Phys. Lett.*, vol. 77, pp. 3325–3327, 2000.

[14] T. W. Berg, S. Bischoff, I. Magnusdottir, and J. Mork, "Ultrafast gain recovery and modulation limitations in self-assembled quantum-dot devices," *IEEE Photon. Technol. Lett.*, vol. 13, pp. 541–543, June 2001.